Nuzzer: A Large-Scale Device-Free Passive Localization System for Wireless Environments

Moustafa Seifeldin, *Student Member, IEEE*, Ahmed Saeed, Ahmed E. Kosba , Amr El-Keyi, *Member, IEEE* and Moustafa Youssef, *Senior Member, IEEE*

Abstract—The widespread usage of WLANs and mobile devices has fostered the interest in localization systems for wireless environments. The majority of research in the context of wireless-based localization systems has focused on device-based active localization, in which devices are attached to tracked entities. Recently, device-free passive localization (*DfP*) has been proposed where the tracked entity is neither required to carry devices nor to participate actively in the localization process. Previous studies have focused on small areas and/or controlled environments. In this paper, we present the design, implementation and analysis of *Nuzzer*, a large-scale DfP localization system, which tracks entities in real environments, rich in multipath. We first present probabilistic techniques for DfP localization of a single entity and evaluate their performance both analytically and in typical office buildings. Our results show that *Nuzzer* gives location estimates with less than 2 meters median distance error. We then give an algorithm for estimating the number of entities in an area of interest and localizing them into coarse-grained zones to enhance the scalability of the system. This indicates the suitability of *Nuzzer* to a large number of application domains.

Index Terms—Device-free localization, multiple entities detection, passive radio map.

1 INTRODUCTION

With mobile devices and wireless networking becoming more and more pervasive in our daily lives, context-aware applications have gained huge interest. As one of the main context information, location determination has been an active area of research. Therefore, many localization systems have been proposed, including the GPS system [3], ultrasonic-based systems [15], infrared-based systems (IR) [19], and RF-based systems [1]. All these systems share the requirement of attaching a device to the tracked entity. Recently, we proposed the device-free passive localization (*DfP*) concept [27]. A *DfP* system provides the capability of tracking entities not carrying any devices nor participating actively in the localization process. This is particularly useful in applications such as intrusion detection, border protection, low cost surveillance, and smart homes automation.

The *DfP* concept is based on the idea that the existence of an entity, e.g. a human, in an RF environment affects the RF signals. This is true for a wide range of frequencies [6], [28] including the 2.4 and 5 GHz bands common in wireless data networks, such as WiFi and WiMax. Even if the person is not obstructing the LOS between the transmitter and the receiver, his/her presence in a wireless environment affects the RSS at the receiver. This is due to absorbing the RF signal as well as affecting the multipath propagation of RF waves.

A typical *DfP* system consists of: (1) signal transmitters, such as access points (APs) and stations used in typical WiFi deployments, (2) monitoring points (MPs), such as standard laptops and wireless-enabled desktops, along with (3) an application server (AS) for processing and initiating actions as needed. Figure 1 shows an example of a DfP system.

In this paper, we present the design, implementation and analysis of *Nuzzer*, a ***large-scale*** device-free passive localization system for ***real*** environments, rich in multipath.

Although *Nuzzer* can operate in both indoor and outdoor environments, we focus on the indoor environments, in which LOS paths from the transmitters to the receivers are usually obstructed by walls. In addition, indoor environments contain substantial amounts of metal and other reflective materials that affect the propagation of RF signals in non-trivial ways, causing severe multipath effects. Generally, reflection, refraction, diffraction, and absorption of RF signals result in multipath fading, which may either decrease or increase the RSS at the MPs. Moreover, RF signals are also affected by noise, interference from other sources, e.g. microwave ovens, and interference between channels. This makes the problem of indoor localization challenging, especially for the *DfP* case.

Nuzzer aims at achieving specific goals:

- **High Accuracy:** The higher the accuracy of a localization system, the more its applications. Our results show that *Nuzzer*'s accuracy is comparable to active RF-based localization, with a median distance error of less than 1.82 meters in two typical office buildings.
- **Ubiquitous Coverage:** Since *Nuzzer* works with the standard wireless data networks and does not require any special hardware, it inherits the ubiquity of the technology it works with, such as WiFi.

- *Moustafa Seifeldin and Amr El-Keyi are with the Wireless Intelligent Networks Center (WINC), Nile University, Cairo, Egypt. E-mail: moustafa.sefeldin@nileu.edu.eg, aelkeyi@nileuniversity.edu.eg*
- *Ahmed Saeed and Moustafa Youssef are with the Department of Computer Science and Engineering and the Wireless Research Facility, Egypt-Japan University of Science and Technology (E-JUST), Alexandria, Egypt. E-mail: ahmed.saeed@ejust.edu.eg, moustafa.youssef@ejust.edu.eg*
- *Ahmed E. Kosba is with Department of Computer and Systems Engineering, Alexandria University, Alexandria, Egypt. E-mail: ahmed.kosba@alexu.edu.eg*

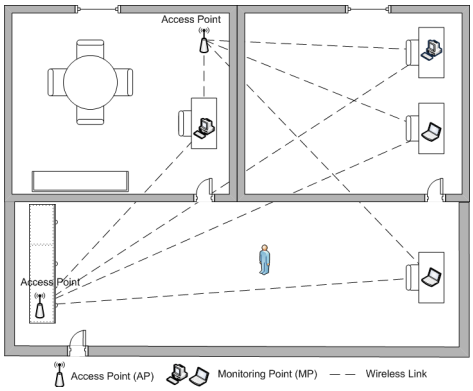

Fig. 1. An example of the different components of a device-free passive localization system in a typical office environment.

- **Scalability:** *Nuzzer* targets typical office buildings with relatively large areas. As an RF-based system, *Nuzzer* has more ubiquitous coverage compared, for example, to systems like computer vision based techniques that require clear field of view to the tracked objects, or IR-based techniques that need LOS between the transmitters and receivers. *Nuzzer* targets *DfP* systems in large scale typical environments with non-LOS localization.
- **Operation in Real Environments:** *Nuzzer* addresses *DfP* localization in typical environments. In a typical wireless environment, the signal power level shows clear temporal and spatial variability [25]. Temporal variability is mainly caused by motion of entities, while spatial variability is caused by multipath fading. Figure 2 shows examples of the RSS in controlled and real environments. Raw streams and histograms show that the RSS has a higher variability in real environments. These variabilities make the localization process more challenging in real environments.
- **Low Cost and Ease of Deployment:** *Nuzzer* uses the same hardware installed for the data network to perform *DfP* localization. This enhances the value of the data network and reduces the cost of deployment.

1.1 Approach

In order to perform localization, we need to capture the behavior of the signal strength when a human is present at different locations in the area of interest. Since this behavior is very complex in indoor environments [23], we do this using a "**passive**" radio map. A radio map is a structure that stores information of the signal strength at different locations in the area of interest [24], [26]. This is usually constructed only once during an offline phase.

During the online phase, the *Nuzzer* system uses the signal strength samples received from the APs at the monitoring points and compares them to the passive radio map to estimate the location of the tracked entity.

Radio map based techniques used in device-based active localization can be categorized into two broad categories: deterministic techniques and probabilistic techniques. Deterministic techniques, represent the signal strength of an AP at a certain location by a scalar value, such as the mean value. Then non-probabilistic approaches are used to estimate the location of the tracked entity. For example, in the RADAR system [1] nearest neighborhood techniques are used to infer the user location. On the other hand, probabilistic techniques, e.g. [25], store information about the signal strength distributions from the APs in the radio map. Then probabilistic techniques are used to estimate the location of the tracked entity. Probabilistic techniques for device-based active localization systems are known to give better accuracy.

In the *Nuzzer* system, we propose probabilistic techniques to implement *DfP* localization in large-scale real environments and show how they differ from device-based active localization techniques. We also propose techniques for estimating the number of entities moving in the same building, and localize them to coarse-grained zones to enhance the scalability of the system. The system performance is evaluated through analysis and implementation in real testbeds.

1.2 Paper Organization

Section 2 presents the different algorithms used in the *Nuzzer* system to track a single entity and the difference between device-based and device-free localization. Section 3 analyzes the system and discusses the effect of the different parameters on performance. Section 4 presents the evaluation of the *Nuzzer* system in large-scale typical office environments and the effect of the different parameters on performance. In Section 5, we propose a technique for estimating the number of entities in the area of interest and localizing them to zones. We discuss different aspects of the *Nuzzer* system and give directions for future work in Section 6. Section 7 presents a comparison between *Nuzzer* and related work. Finally, Section 8 concludes the paper.

2 The Nuzzer System

In this section, we present the different algorithms used in the *Nuzzer* system. We start by an overview of the system followed by a description of our probabilistic algorithms.

2.1 Overview

The *Nuzzer* system works in two phases:

1) Offline phase: where we build the passive radio map. A passive radio map is similar to the active radio map usually used in device-based active WLAN location determination systems, such as [1], [2], [25]. However, in an active radio map, a user stands with a device at the radio map locations and collects samples from all the APs in range. On the other hand, for the passive radio map construction, a person stands at the radio map locations not carrying any device and his effect on the different data streams received at the MPs is recorded. Figure 3 demonstrates the difference between active and passive radio map construction. In a passive radio map, we have a histogram per raw data stream, as compared

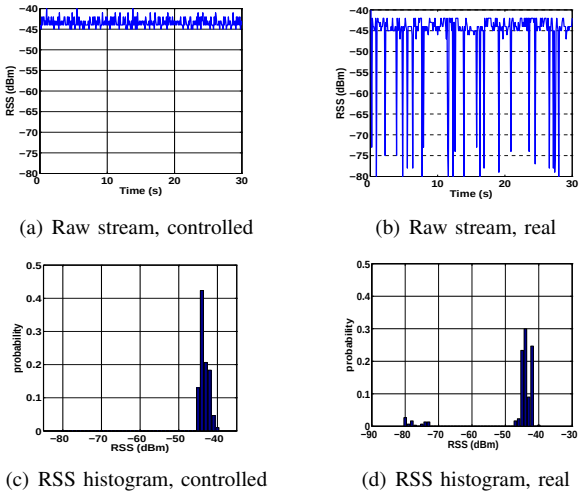

(a) Raw stream, controlled (b) Raw stream, real

(c) RSS histogram, controlled (d) RSS histogram, real

Fig. 2. RSS behavior in a controlled versus a real environment.

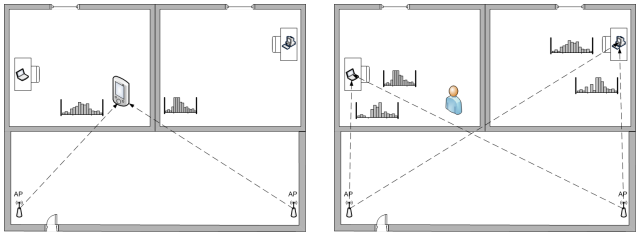

(a) Active (b) Passive

Fig. 3. Difference between active and passive radio maps' construction.

to a histogram per AP. Also, a person does not carry any device when constructing the passive radio map.

2) Online phase: where we estimate the number of persons in the area of interest and the "zones" they are located in (Section 5). We then track the person location within each zone based on the RSS from each data stream and the passive radio map prepared in the offline phase.

We define two modes of operation for the online phase: The Discrete Space Estimator and the Continuous Space Estimator.

1) The Discrete Space Estimator module returns the radio map location that has the maximum probability given the received signal strength vector from different streams. Therefore, the output of the discrete space estimator must be one of the calibrated locations.
2) The Continuous Space Estimator works as a post processing step after the discrete space estimator and tries to return a more accurate estimate of the person location in the continuous space. Therefore, if a person is standing between two radio map locations, the continuous space estimator should provide a better estimate than the discrete space estimator.

We start by presenting our mathematical model followed by details of the two modes of operation.

2.2 Mathematical Model

Without loss of generality, let $\mathbb{X}$ be a two dimensional physical space. Let n represent the total number of data streams in the system (number of APs multiplied by number of MPs). We denote the n-dimensional signal strength space as $\mathbb{N}$. Each element in this space is a n-dimensional vector whose entries represent the signal strength readings from different streams, where each stream represents an (access point, monitoring point) pair. We refer to this vector as s. We also assume that the samples from different APs are independent and hence, the samples of different streams are independent. A person standing at any location $x \in \mathbb{X}$ affects the signal received at the different MPs, and hence the equivalent n-dimensional vector.

Therefore, the problem becomes, given a signal strength vector $s = (s_1, ..., s_n)$ received in the online phase, we want to find the location $x \in \mathbb{X}$ that maximizes the probability $P(x|s)$.

In the next section, we assume a discrete space $\mathbb{X}$. We discuss the continuous space case in Section 2.4.

2.3 Discrete Space Estimator

During the offline phase, *Nuzzer* estimates the signal strength histogram for each stream corresponding to the person standing at each radio map location. For example, when a person stands at a specific radio map location x, the system collects signal strength samples for each stream (Figure 3(b)). Using these signal strength samples, a histogram for each stream i is constructed independently that represents the probability $P(s_i|x)$ (see e.g. Figure 2). Therefore, at each radio map location, we have a set of histograms representing the signal strength received from each stream when the person stands at this location.

Now, consider the online phase. A person is standing at an unknown location x leading to a received signal strength vector $s = (s_1, ..., s_n)$. Given s, we want to find the location $x \in \mathbb{X}$ that maximizes the probability $P(x|s)$, i.e., we want $\arg\max_x P(x|s)$

Using Bayes' theorem, this can be written as:

$$x^* = \arg\max_x P(x|s) = \arg\max_x [\frac{P(s|x).P(x)}{P(s)}] \quad (1)$$

Assuming that all locations are equally probable[1], the term $P(x)$ can be factored out from the maximization process in Equation 1. Also, since $P(s)$ is independent of x, it can be factored out too. This yields:

$$x^* = \arg\max_x [P(x|s)] = \arg\max_x [P(s|x)] \quad (2)$$

$P(s|x)$ can be calculated for each radio map location x using the histograms constructed during the offline phase as:

$$P(s|x) = \prod_{i=1}^{n} P(s_i|x) \quad (3)$$

1. If the entity's profile, $P(x)$, is known, i.e. the probability of the entity being at each of the radio map locations, it can be used in Equation 1.

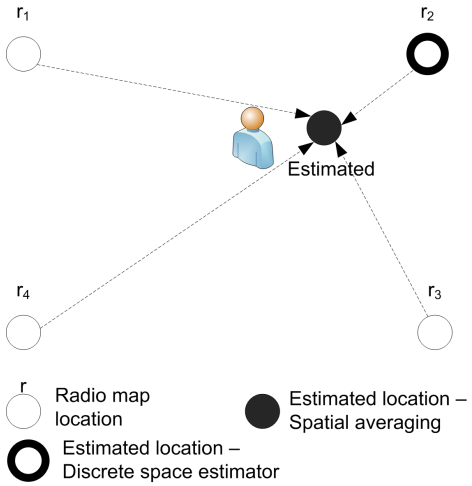

Fig. 4. An example of using the spatial averaging technique to enhance accuracy.

The above equation considers only one sample from each stream for a location estimate. In general, a *number of successive samples*, m, from each stream can be used to improve performance[2].

In this case, $P(s|x)$ can then be expressed as follows:

$$P(s|x) = \prod_{i=1}^{n} \prod_{j=1}^{m} P(s_{i,j}|x) \quad (4)$$

where $s_{i,j}$ represents the j^{th} sample from the i^{th} stream.

Thus, given the signal strength vector s, the discrete space estimator returns the location x that has the maximum probability using Equation 4.

2.4 Continuous Space Estimator

The discrete space estimator returns a single location from the set of locations in the passive radio map. In general, an entity need not be standing at one of the radio map locations. Therefore, to increase the system accuracy, *Nuzzer* uses spatial and time averaging techniques to obtain a location estimate in the continuous space.

2.4.1 Spatial averaging

This technique is based on treating each location in the radio map as an object in the physical space whose weight is equal to the probability assigned by the discrete space estimator, normalized so that the sum of probabilities equals one. We then obtain the center of mass of the k objects with the largest mass, where k is a system parameter, $1 \leq k \leq \| \mathbb{X} \|$. Figure 4 shows an example of using the spatial averaging technique. The discrete space estimator will return the location r_2, assuming it is the closest in the signal strength space to the actual person location. Using the spatial averaging technique, a better location estimate can be obtained by calculating the center of mass of the top 4 locations ($k = 4$).

More formally, let $P(x)$ be the probability of a location $x \in \mathbb{X}$, i.e., the radio map, and let $\overline{\mathbb{X}}$ be the list of locations in the radio map *ordered* in a descending order according to the normalized probability assigned from the discrete space estimator. The center of mass technique estimates the current location x as:

$$x = \frac{\sum_{i=1}^{k} P(i).\overline{\mathbb{X}}}{\sum_{i=1}^{k} P(i)} \quad (5)$$

Note that the estimated location x need not be one of the radio map locations.

2.4.2 Time averaging

This technique uses a time averaging window to smooth the resulting location estimates. The technique obtains the location estimate by averaging the last w location estimates obtained by either the discrete space estimator or the spatial averaging estimator.

More formally, given a stream of location estimates $x_1, x_2, ..., x_t$, the technique estimates the current location $\overline{x_t}$ at time t as:

$$\overline{x_t} = \frac{\sum_{i=t-min(w,t)+1}^{t} x_i}{min(w,t)} \quad (6)$$

The length of the time averaging window affects the latency and accuracy of the system as discussed in Section 4.

3 System Analysis

In this section, we present an analytical model for the probabilistic algorithm suggested in Section 2 and discuss the effect of different system parameters on performance.

3.1 Assumptions

- The area of interest, $\mathbb{X}$, is covered by n streams and contains L radio map locations.
- The effect of a person standing at a particular location in the radio map on the RSS of a stream can be modeled by a Gaussian random variable whose mean depends on the specific location the person is standing at but whose **variance is independent of the person location** and depends only on the stream. Therefore, the radio map at location $x \in \mathbb{X}$, f_x, is represented as a vector $f_x = [\zeta_{x_1}, \zeta_{x_2}, ..., \zeta_{x_n}]$ where $\zeta_{x_i} = (\mu_{x_i}, \sigma_i^2)$ and μ_{x_i} and σ_i^2 are the true mean and variance respectively of the Gaussian random variable representing the RSS distribution of the i^{th} data stream when a human is present at location x.
- The signal strength values from all streams are mutually independent.

3.2 Probability of Correct Estimation

In this section, we derive an expression for the probability of correct estimation which is the probability of correctly estimating the **exact** person location. Based on Equation 3, the discrete space estimator calculates the probability $P(s|x)$

2. These samples are extracted from consecutive beacons.

of the entity standing at location $x \in \mathbb{X}$ given a measured signal vector s. The location with the highest such probability is chosen as the estimated location.

Consider two-locations (τ and $\upsilon \in \mathbb{X}$). Assuming that an entity is present at the first location τ, the following inequality must hold for the algorithm to correctly estimate the entity's location:

$$P(s|\tau) > P(s|\upsilon)$$

$$\Rightarrow \prod_{i=1}^{n} e^{\frac{-(s_i-\mu_{\tau i})^2}{2\sigma_i^2}} \geq \prod_{i=1}^{n} e^{\frac{-(s_i-\mu_{\upsilon i})^2}{2\sigma_i^2}}$$

$$\Rightarrow \sum_{i=1}^{n} \frac{(s_i-\mu_{\upsilon i})^2}{2\sigma_i^2} - \sum_{i=1}^{n} \frac{(s_i-\mu_{\tau i})^2}{2\sigma_i^2} \geq 0 \quad (7)$$

$$\Rightarrow \sum_{i=1}^{n} \frac{s_i(\mu_{\tau i}-\mu_{\upsilon i})}{\sigma_i^2} + \sum_{i=1}^{n} \frac{\mu_{\upsilon i}^2-\mu_{\tau i}^2}{2\sigma_i^2} \geq 0 \quad (8)$$

Let $z_\upsilon = \sum_{i=1}^{n} \frac{s_i(\mu_{\tau i}-\mu_{\upsilon i})}{\sigma_i^2} + \sum_{i=1}^{n} \frac{\mu_{\upsilon i}^2-\mu_{\tau i}^2}{2\sigma_i^2}$. z_υ is a Gaussian random variable with mean μ_{z_υ} and variance $\sigma_{z_\upsilon}^2$ equal to:

$$\mu_{z_\upsilon} = \sum_{i=1}^{n} \frac{\mu_{s_i}(\mu_{\tau i}-\mu_{\upsilon i})}{\sigma_i^2} + \sum_{i=1}^{n} \frac{\mu_{\upsilon i}^2-\mu_{\tau i}^2}{2\sigma_i^2}$$

$$\sigma_{z_\upsilon}^2 = \sum_{i=1}^{n} \frac{(\mu_{\tau i}-\mu_{\upsilon i})^2}{\sigma_i^2}$$

The probability of correctly estimating the true location when comparing only two locations could be expressed as $Pr\{z_\upsilon > 0|\tau\}$. For a radio map with L locations, the probability of correctly estimating the location τ, $P(\text{Correct}|\tau)$, given a measured signal vector s, can be expressed as

$$P(\text{Correct}|\tau) = Pr\{z_{l_1} > 0|\tau, z_{l_2} > 0|\tau, \ldots, z_{l_{L-1}} > 0|\tau\} \quad (9)$$

Where $\{l_i\}$ is the set of all radio map locations other than τ. Therefore, the overall probability of correct estimation, $P(\text{Correct})$ can be expressed as

$$P(\text{Correct}) = \sum_{\tau=1}^{L} P(\text{Correct}|\tau)P(\tau)$$

Without loss of generality and assuming all locations are equi-probable, then

$$P(\text{Correct}) = \frac{1}{L}\sum_{\tau=1}^{L} P(\text{Correct}|\tau) \quad (10)$$

3.3 Discussion

Note that the effect of the number of streams appears from the parameter n in Equation 7 while the effect of the number of locations in the radio map (parameter L), and hence the grid spacing, appears in Equation 9. From Equation 7 we see that, when the number of locations in the radio map is fixed, increasing the number of streams will increase the LHS of the equation, since the measurement s_i from the additional stream, on average, will be closer to the mean μ_{τ_i} than to μ_{υ_i}. This will increase the probability of correct detection and consequently, decrease the average distance error.

Equation 9 shows that fixing the area of interest and increasing the number of radio map locations L, i.e. reducing the grid spacing, will reduce the value of the joint probability $P(\text{Correct}|\tau)$ as we have more terms. This is intuitive as reducing the grid spacing will make more locations closer in both the physical and RSS space, reducing the probability of correct detection.

However, for the average distance error, we have two opposing factors as L increases: (1) the probability of error increases as discussed in the previous paragraph and (2) the distance between locations decreases, reducing the distance error. This means that the average distance error may increase or decrease as L increases. As we show through numerical evaluation and actual implementation, the probability of error effect is minimal. This leads to decreasing the average distance error as L increases.

3.4 Numerical Validation

In this section, we numerically validate the model given in Section 3.2 under the same assumptions. For capturing the human effect on the signal strength, we used the Fresnel-Kirchhoff Diffraction model [14] which associates the dimensions of an obstacle, e.g. the human, and its location to the effect it has on signal strength of the stream. Figure 5 shows the used topology.

Figure 6 shows the effect of increasing the number of streams on the probability of error and average distance error. The figure shows that increasing the number of streams n has a positive effect on both quantities as discussed in Section 3.3.

Figure 7 shows the effect of increasing the number of calibrated locations L, i.e. decreasing grid spacing, on accuracy. The figure shows that increasing L has a negative impact on the probability of error and a positive impact on the average distance error. This is in accordance with our analysis in this section.

4 Performance Evaluation

In this section, we study the performance of the proposed discrete space estimator and continuous space estimator in two typical office environments. We start by describing the experimental setup and data collection, followed by studying the effect of different parameters on the performance of the proposed techniques. We also compare the performance of our system to two other estimators:

1) A random estimator: this is used as a baseline for performance comparison. A random estimator selects a

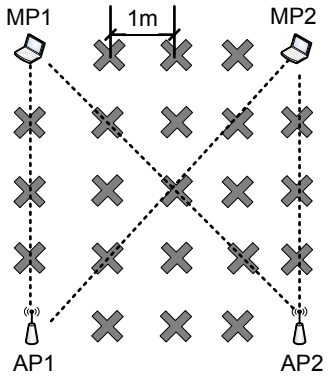

Fig. 5. Topology for the numerical results experiment.

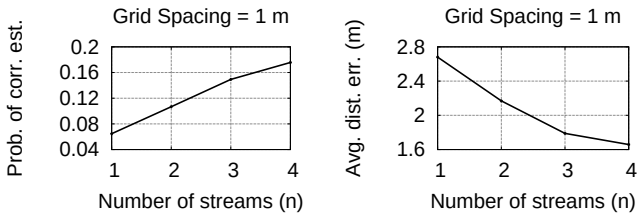

(a) Prob. of correct est. (b) Avg. dist. error

Fig. 6. The effect of changing the number of streams on performance for the numerical results.

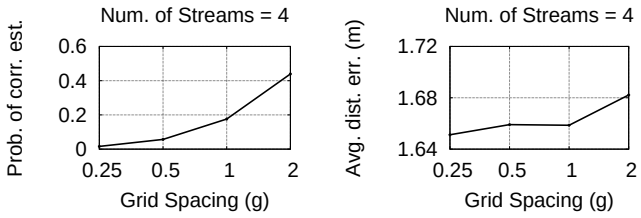

(a) Prob. of correct est. (b) Avg. dist. error

Fig. 7. The effect of changing the grid spacing on performance for the numerical results.

random location in the area of interest as its estimate, without using the signal strength information.

2) A deterministic technique: This estimator stores in the radio map the average signal strength from each stream at each location. During the online phase, the deterministic estimator returns the radio map location whose stored signal strength vector is closest, in signal strength space, to the received vector. More details about this technique can be found in [17].

4.1 Experimental Testbeds

We performed two experiments in two different testbeds to evaluate the system. Due to space constraints, we will present the performance analysis of the system for the first testbed in detail in the next subsections, and then summarize the performance results of the second testbed.

The first experimental testbed is located in the first floor of a two-storey typical office building (Figure 8). The floor

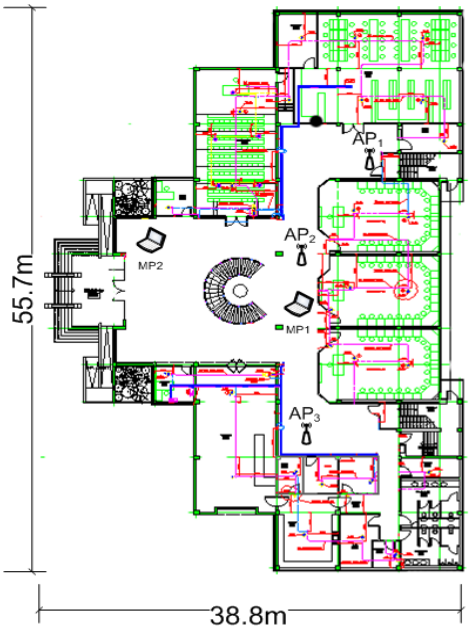

Fig. 8. Floor plan of the area where the *DfP* experiment was performed.

has an area of 750 m^2 (about 8000 sq. ft.). The experiment was carried out in the main entrance and the corridors, where there were furniture, plants, and substantial amount of metal. This experiment was conducted in an 802.11b environment. The building had ten Cisco APs (model 1130). We also used two different laptops; one Dell Latitude D830, and one HP Pavilion ze5600 laptop. The two laptops had Orinoco Silver cards attached to them. APs represent the transmitting units, while laptops represent the MPs. Figure 8 shows the locations of APs and MPs.

Since our experiments show that the performance saturates when the number of APs exceeds three, we only report here the accuracy using only the three APs indicated in Figure 8. These APs are the ones with the best coverage in the testbed area.

The second experiment was conducted in the second floor of an office building with an area of 130 m^2 (about 1400 sq. ft.). The floor was covered with typical furniture. The layout is shown in Figure 18. Similarly, only six streams were only used for the tracking experiment (i.e. APs: 1 and 2, MPs: 1, 2 and 3). The hardware used in this experiment was different from the one used in the first testbed. The devices in this testbed included TP-link TL-WA500G access points and D-Link Airplus G+ DWL-650 wireless NICs. The performance of the system under this testbed is summarized in Section 4.6.

4.2 Data Collection

The wireless cards measure different physical signals during the experiment, such as signal strength and noise. We use only the received signal strength indicator (RSSI) values, reported in units of dBm, which is known to be a better function of distance than noise [1]. We collected samples from the access

TABLE 1
Tunable parameters used in our experiments

Parameter	Default value	Meaning
n	6	Number of processed raw data streams
m	26	Number of consecutive samples to use from one stream per location estimate
g	2m	Grid spacing
k	2	Number of locations to average in the spatial averaging technique
w	5	Size of the time averaging window

points at the rate of five samples per second[3].

For the first testbed, each one of the two MPs records samples from the three APs, giving a total of six data streams (one stream for each (MP, AP) pair) for both testbeds. During the offline phase, a person stands at each of 53 different radio map locations, spaced 2m apart, with a fixed orientation [4] and we record the samples for 60 seconds for each of the six data streams, giving a total of 300 samples per stream.

For testing purposes (online phase), we collected another ***independent*** test set at 32 locations. The test set was collected at a different time from the training set.

4.3 System Parameters and Metrics

For the discrete space estimator, we can tune the number of consecutive samples to use from each stream (m), the number of raw data streams to use (n), and the grid spacing (g).

For the continuous space estimator, in addition to these three parameters, we can tune the number of locations to use in the spatial averaging (k) and the length of the window to use for time averaging (w). Table 1 summarizes the parameters used in our system. Unless otherwise specified, we use the default parameters valueswhich give the best combined performance.

We also use the median distance error and the CDF of distance error as our two performance metrics.

4.4 Discrete Space Estimator

We start by studying the effect of the different parameters on performance. Then we compare the discrete space estimator to other techniques. Due to space constraints, we show only the results for the median distance error noting that the results for the probability of correct estimation exhibits similar performance.

4.4.1 Impact of the number of samples per stream

Figure 9 shows the effect of increasing the number of samples used from each stream per location estimate on the accuracy of the system (parameter m). The figure shows that, as expected, the median distance error decreases as m increases. However, as m increases, the latency, i.e. time required per location estimate, of the system increases as we have to wait till we collect the m samples. Therefore, a balance is required between the accuracy and latency of the system. This depends on the specific deployment environment. Moreover, Adaptive sampling techniques can be used, if needed. Another approach is to use a moving window of m samples, where at each estimate, one new sample is added to $m-1$ old samples. This removes the requirement of waiting for m samples.

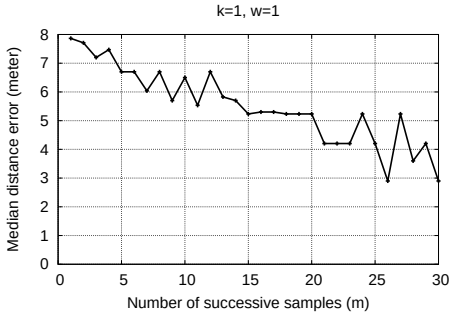

Fig. 9. Median distance error of the discrete space estimator for different values of the number of successive samples from each stream per location estimate (m).

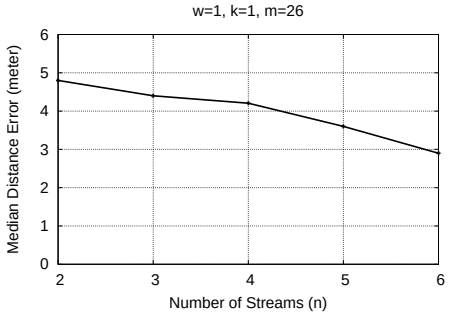

Fig. 10. Median distance error of the discrete space estimator versus the number of used raw data streams (n).

4.4.2 Impact of the number of streams

Figure 10 shows the median distance error versus the number of streams (n) used in the estimation process. For a specific n, we plot the best result over all possible $\binom{6}{n}$ combinations of streams. The figures show that as the number of streams increases, we have more information about the environment, and thus we can obtain better accuracy.

4.4.3 Impact of the grid spacing

Figure 11 shows the effect of increasing the grid spacing on the accuracy of the system (parameter g). The figure shows that as the grid spacing increases, the accuracy degrades until it saturates.

3. According to the 802.11 standard, WiFi access points typically transmit 10 beacons per second. Since the sampling frequency is much higher than the human motion rate, the accuracy of the system is not affected under typical sampling rates. We confirmed this through our experiments. Note that the MPs run in passive monitoring mode, i.e. they do not incur any additional traffic on the network. Moreover, as the typical operation environment for the system is to run when there is no one inside the area of interest, the network is under-utilized and the overhead of transferring the data to the processing server, over the **wired** interface, is practically negligible.

4. Our experience with the system shows that the system performance is not sensitive to the person orientation.

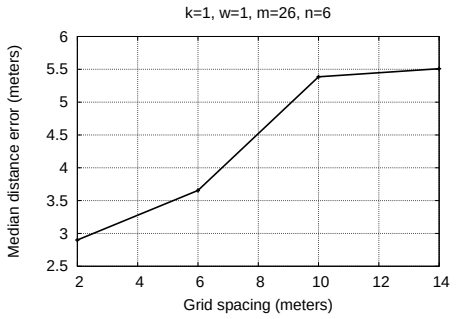

Fig. 11. Median distance error of the discrete space estimator versus the grid spacing (g).

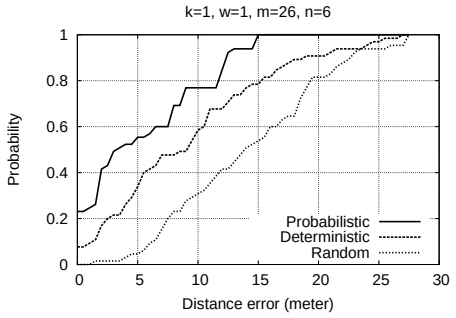

Fig. 12. CDFs of the Euclidean distance between actual locations and locations estimated by the *discrete space* estimator technique.

4.4.4 Comparison with other techniques

Figure 12 shows the cumulative distribution function (CDF) of the distance error using the discrete space estimator, a deterministic estimator, and a random estimator.

We can see from the figure that the median distance error of the discrete space estimator is 2.9m meters, 2.9 times better than deterministic techniques and 4.8 times better than the random estimator. This ratio is even more for the lower percentile values.

The value of the CDF at zero distance error indicates the probability of determining the exact location. Probabilistic techniques demonstrate superiority over deterministic techniques as they use the entire signal strength distribution, rather than just the average.

4.5 Continuous Space Estimator

We start by studying the performance of the spatial and time averaging techniques followed by a comparison with the deterministic and random estimators.

4.5.1 Spatial averaging

Figure 13 shows the effect of increasing the number of neighbors used in the spatial averaging process (k) on the median distance error. The figure shows an improvement of 10% between $k = 1$ and $k = 3$ after that the performance saturates. Therefore, setting k to be the total number of locations in the radio map will give the best accuracy, regardless of the area

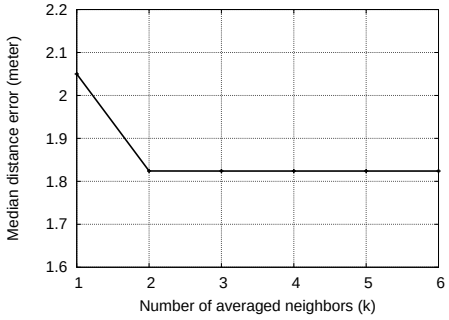

Fig. 13. Median distance error of the continuous space estimator versus the number of neighbors used in the spatial averaging (k).

of interest, with minimal effect on the running time of the algorithm.

4.5.2 Time averaging

Figure 14 shows the effect of increasing the size of the time averaging window (w) on the median distance error. The figure shows an improvement of 65% between $w = 1$ to $w = 5$. Again, we have a tradeoff between accuracy and latency. The higher the value of w, the higher the accuracy and the higher the latency. Therefore, the specific value of w depends on the application in use.

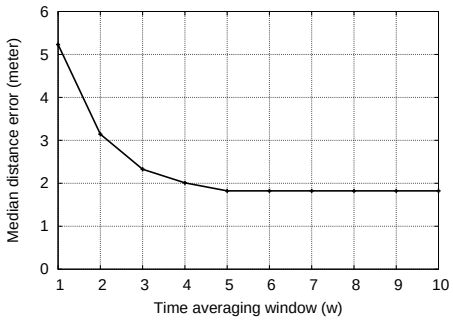

Fig. 14. Median distance error of the continuous space estimates versus the time averaging window size (w).

4.5.3 Comparison with other techniques

Figure 15 shows the cumulative distribution function (CDF) of the distance error using the continuous space estimator for the best values of the parameters. We can see from the figure that the median distance error of the continuous space estimator is ***1.82*** meters, 3.7 times better than deterministic techniques and 7.7 times better than the random estimator.

4.6 System Performance for Testbed 2

In this section, we summarize the system performance for Testbed 2 (Figure 18). In this testbed, 38 locations were selected for collecting training data covering all the floor with a grid spacing of 1.8m, and 21 locations were selected for collecting the independent test set. We also use the same values for the parameters m, k and w used for Testbed 1

	Area	Number of streams	Number of training locations	Number of testing locations	Grid spacing	25^{th} percentile	50^{th} percentile	75^{th} percentile
Testbed 1	750m^2	6	53	32	2m	0.9m	1.82m	9.3m
Testbed 2	130m^2	6	38	21	1.8m	0.0m	0.85m	5.2m

TABLE 2
System Performance for testbeds 1 and 2.

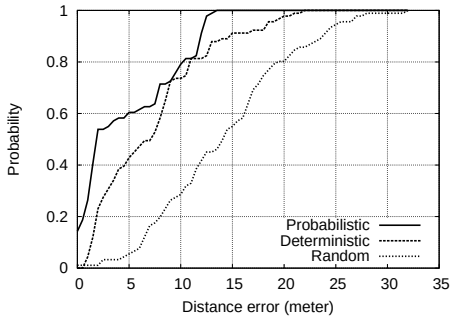

Fig. 15. CDFs of the Euclidean distance between actual locations and locations estimated by *continuous space* estimation technique.

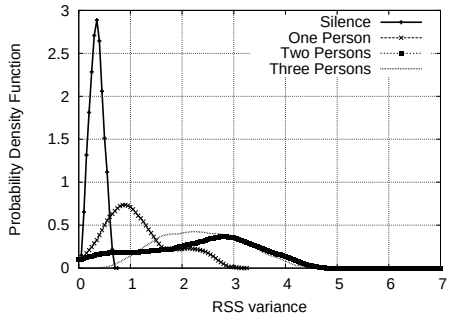

Fig. 16. PDFs of the RSS variance when multiple entities cut the LOS between a transmitter and a receiver.

(Table 1). The results are summarized in Table 2. Comparing the results for both testbeds, it can be noted that the distance error percentiles of the second testbed are less than those of the first testbed. This is because the area of the second testbed is less than the area of the first testbed. In addition, the grid spacing between the locations of the second testbed is lower than the first testbed. This is consistent with the analysis in Section 3. This also highlights that the system is robust to changes in the hardware configuration due to using a radio map based technique.

4.7 Summary

In this section, we showed that using only six data streams, the *Nuzzer* system provides a *non-LOS DfP* localization system capable of covering large areas, rich in multipath, with very high accuracy; 1.82 meters median distance error in the first testbed and 0.85 meters in the second one. This accuracy is not as high as the accuracy reported for device-based active localization systems (0.5 meters in [25]). However, it is still suitable for many applications.

Comparing the performance of the continuous space estimator to the discrete space estimator for the first testbed, we find that the median distance error in the discrete space is 2.9 meters, whereas in the continuous space, the median is 1.82 meters, 37% better.

The spatial averaging and temporal averaging techniques are independent and can be used together to further enhance performance. Combining all techniques, leads to the above mentioned accuracy.

The system parameters m and w, which represent the number of samples from each stream and the time averaging window size respectively, can be tuned to balance accuracy and latency, depending on the deployment environment.

We also showed that the implementation results show the same trend as the analysis in Section 3. The difference between the values is due to the difference in assumptions between the model and the real world. This validates our analysis.

The results also showed that the *Nuzzer* system can provide very good accuracy, outperforming the deterministic approach by 3.7 times, even when the number of available data streams is low. This shows the usability of the system in environments with limited hardware installment, such as in homes.

5 Handling Multiple Entities

The previous section proved the feasibility of tracking a single entity in the area of interest. In this section, we address the problem of multiple entities identification and coarse-grained localization (zone localization). Identification refers to determining the number of entities while coarse-grained localization refers to determining the zones in the area of interest where the multiple entities are located. Once this identification and initial localization are performed, the techniques described in Section 2 can be applied to each zone to determine a more accurate location for the multiple entities. We describe statistical techniques, based on the variance of the received signal strength of different streams, for the identification and coarse-grained localization of multiple entities.

The rest of this section is organized as follows. We start by motivating our approach and describing the evaluation testbeds in sections 5.1 and 5.2 respectively. In Section 5.3, we describe a technique for estimating the number of entities in a building. Finally, in Section 5.4, we propose a technique for localizing multiple entities to different zones.

5.1 Overview

Figure 16 shows the PDF of the RSS variance of one stream during the silence period and when one or more entities are

moving randomly in the area covered by that stream. This experiment was conducted in an area of 15.3 m^2, where the distance between the AP and MP was 3.4m.

We can see from the figure that:

- The RSS variance distribution of the stream during the silence period can be clearly distinguished from the case when an entity is present with high probability.
- The mean of the variance when one or more entities exist on the LOS (${\sigma_{\text{on}}}^2$) is higher than the mean of the variance of RSS of the stream during his/her absence (${\sigma_{\text{off}}}^2$).
- The high degree of overlapping between the variance distribution of the different cases of human existence indicates that we cannot clearly distinguish between the number of entities based on the variance of one stream only.

In the next two subsections, we leverage these observations to develop techniques for identifying the number of entities and localize them to within zones in the area of interest based on the variance of the different streams in the area of interest.

5.2 Testbeds

To evaluate the proposed techniques, we conducted two experiments. In general, a zone can be specified using different techniques. For example, each room/logical area can be assigned to a zone (Testbed 2). Similarly, zones can be assigned based on the streams passing through them (Testbed 1).

The first experiment was in a curved corridor with an area of about 24 square meters (Figure 17). The area is divided into five zones according to the locations of three APs and four MPs. The second experiment was performed in a larger area in the second floor of an office building (Figure 18), where the area (130 square meter) is divided into six zones. To test the system capability, the configuration of Testbed 2 was selected such that the LOS paths between the APs and MPs are obstructed by walls. Also, Zone 2 is just indirectly covered by the AP1-MP3 and AP2-MP3 streams and contains neither APs nor MPs.

The RSS for each stream i is recorded during an offline phase to calculate its variance, (${\sigma_{\text{off}i}}^2$), when no person exists in the area. Then, the RSS for each stream is recorded again when a person moves randomly within each of the zones, in order to calculate (${\sigma_{\text{on}i}}^2$). We ran the experiment for different cases when there are two and three entities moving in different zones in the area of interest.

To evaluate the multiple entities algorithms, two sets of experiments were conducted in each testbed. During the first set of experiments two persons move in two of the zones with all possible combinations (i.e. $\binom{5}{2}$ for Testbed 1 and $\binom{6}{2}$ for Testbed 2). During the second set of experiments three persons move in three of the zones with all possible combinations.

5.3 Identifying the Number of Entities

Our approach is based on using the relative variance, i.e. the ratio between the variance of the human presence to silence periods ($\frac{{\sigma_{\text{on}}}^2}{{\sigma_{\text{off}}}^2}$), as a feature for identifying the number of entities. The idea is that as the number of entities in a given

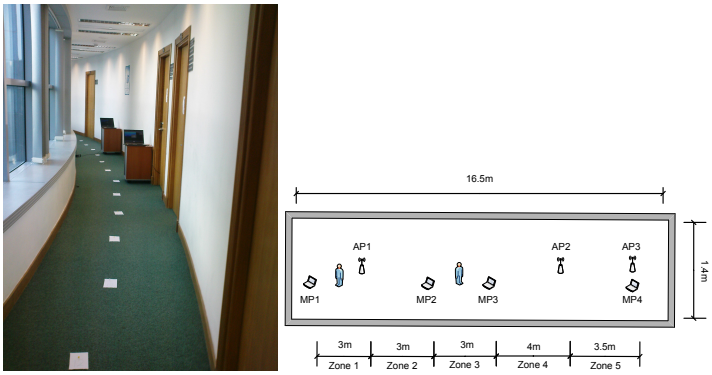

(a) Picture showing non-LOS conditions for part of Testbed 1.

(b) Corridor layout.

Fig. 17. Testbed 1: The corridor is separated by laptops and APs into five zones.

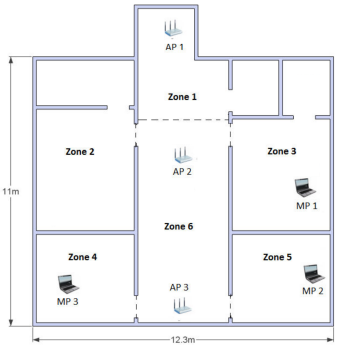

Fig. 18. Testbed 2: The area is divided to six zones. The LOS paths in this layout are obstructed by walls.

area of interest increases, the average relative variance of all streams covering this area also increases. Note that using the entire set of streams, rather than processing every stream independently, is based on the third observation in Section 5.1 that an individual stream cannot differentiate between the number of entities. More formally, let N_s be the number of streams covering the entire area. Therefore, the average relative variance is given by:

$$RV_{\text{av}} = \frac{1}{N_s} \sum_{i=1}^{N_s} \frac{{\sigma_{\text{on}\ i}}^2}{{\sigma_{\text{off}\ i}}^2} \tag{11}$$

The value of RV_{av} is then compared against different thresholds to determine the number of entities. The system declares that there are N entities in the area of interest if $\tau_N < RV_{\text{av}} < \tau_{N+1}$, where τ_N and τ_{N+1} are the N^{th} and the $N+1^{\text{st}}$ thresholds.

Our experiments show that when τ_1 is between 1.5 and 2, τ_2 is between 2 and 3, and τ_3 is between 4 and 5, the system gives good accuracy. Figure 19 shows the CDF of estimation error as compared to a random estimator. The figure shows that the proposed method can achieve 81% accuracy for determining the number of entities in Testbed 1. In addition, the remaining 19% error is always within a difference of one from the actual number of entities in the area of interest. For Testbed 2, the

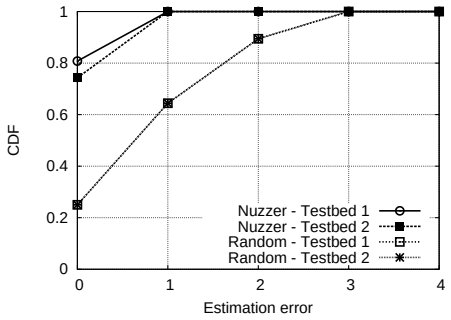

Fig. 19. CDFs of estimation error in identifying the number of entities.

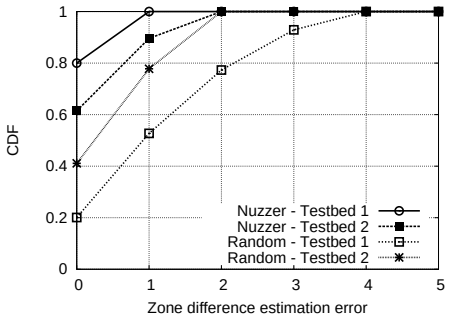

Fig. 20. CDFs of zone difference error for localizing multiple entities. A zone difference of zero means an exact match.

figure shows that the method could achieve 71% exact matches and the remaining 29% error is always within a difference of one. This is due to the less coverage and the larger area of Testbed 2.

5.4 Multiple Entities Zone Localization

Once the number of entities, N, is estimated, we need to determine a rough estimate of where the multiple entities are located. We recursively apply the relative variance approach to the streams passing within each zone, where for this purpose a stream represents the line connecting the AP and MP, to determine whether an entity is located inside this zone or not. More formally, given a zone covered by N_z streams, the average relative variance per zone, $RV_{\text{Zone}_{\text{av}}}$, is calculated as:

$$RV_{\text{Zone}_{\text{av}}} = \frac{1}{N_z} \sum_{i=1}^{N_z} \frac{{\sigma_{\text{on}\ i}}^2}{{\sigma_{\text{off}\ i}}^2} \tag{12}$$

The N zones with the highest relative variance are returned as the estimated zones.

Figure 20 shows the CDF of zone estimation error for both testbeds compared to random estimators. The figure shows that 80% of the estimates are exact with the remaining 20% of the estimates mapped to adjacent zones in Testbed 1. Given the testbed area, this is equivalent to a location estimation error of 3 meters. For Testbed 2, more than 61% of the estimates are exact, whereas about 30% of the estimates were mapped to adjacent zones and the remaining estimates were mapped to more distant zones. The performance degraded in Testbed 2 with repect to Testbed 1, because the area of Testbed 2 is much larger and the LOS paths in Testbed 2 are obstructed by walls. Also, Zone 2 in Testbed 2 is indirectly covered by two streams, and finally there are many common streams between zones in Testbed 2 more than Testbed 1, which leads to confusion between zones.

Note that as indicated before, the techniques presented in Section 2 can be applied within each zone to further enhance the accuracy.

As a final note, we point out that localizing entities to within zones also enhances the scalability of the technique. On one side, zones reduce the computational requirements of the system as it limits the number of radio map locations to be processed. On another side, since each zone is processed using the streams that mainly have an effect in it only, this makes the zones virtually independent from each others. This becomes even more valid as the scale of the environment increases, as the set of APs and MPs covering the area would change. Consequently, the number of sampling points become independent from the number of people as we can calibrate using one person only. In summary, the scalability is enhanced when the system uses the multi-entity detection technique as follows: (1) Identify the number of persons in the environment; (2) Identify the active zones; (3) For each identified active zone, use the technique presented in Section 2 for single person tracking using the streams that are mainly affected in the identified active zone.

6 Discussion

In this section, we discuss different aspects of the *Nuzzer* system and our ongoing work on enhancing the system.

6.1 Automatic Generation of the Passive Radio Map

One of the disadvantages of using a radio map is the effort needed to construct it during the offline phase. To reduce this effort, an RF-propagation tool can be used that takes as an input the floor plan of the area of interest, objects in the environment, their RF characteristics, and locations and characteristics of the APs and MPs and based on that generates the radio map automatically.

Such tool will not be useful only in reducing the ***calibration effort***, but also in understanding the fundamentals of the *DfP* concept and in other functionalities related to tracking such as tracking multiple entities, optimal positioning of APs and MPs, entity identification, suitability for different application domains, as well as dealing with physical size, orientation, and other properties of the passive entity.

Other approaches applied in the context of the device-based active localization systems to reduce the calibration effort, e.g. [11], can also be experimented with.

6.2 Entity Identification

One extension to the work presented in this paper is to obtain more information about the entity. This includes identifying the class, name, size, mass, shape, and/or composition of the

entity. Some of these characteristics may be easier to identify than others, e.g. differentiating a tank from a human in a *DfP* border protection system. In addition to its importance, this identity information can also be used to enhance the performance of the system as a whole, e.g. by changing the operation mode based on the entities' characteristics.

One approach for addressing this extension is by constructing a "*DfP*-profile" for different entities that captures their characteristics and matching them to the profile of identified entities. For example, since different materials have different reflection coefficients, it may be useful to use this property in constructing this profile. Similar ideas have been proposed before for constructing human profiles based on using pressure sensors as in [13]. This opens the possibility for research in this challenging area. Automatic construction of the passive radio map can also help in identifying the features that should be captured by a *DfP*-profile.

6.3 Dynamic Changes in the Environment

Changes in the environment due to the time of day and day of year, such as temperature and humidity, can make the operational environment different from the environment used in constructing the radio map, and hence may reduce accuracy. Note that for the *DfP* problem, changes in people activity patterns should have little effect on the system, as the system typical environment is at periods where no one is expected to be in the area of interest. For environmental changes, based on the experience from the device-based active localization systems [25], their effect is limited. Another possibility is to use multiple radio maps, corresponding to different environmental conditions [2]. An automatic passive radio map construction tool can aid in solving this problem by capturing the effect of these different changes. Our experiments, presented in Section 4, use an independent test set separate from the one collected during the offline phase. This quantifies the effect of the dynamic changes in the environment.

6.4 Using Different Hardware

Another point related to the usability of the system is how the performance of the system is affected with the usage of different APs and MPs hardware. For different APs, we do not expect that this will have much effect on the accuracy as we capture the behavior of the APs at the monitoring points using the passive radio map constructed during the offline phase, instead of assuming a model for the behavior.

For using different wireless cards, there are two cases: (1) The first case is the effect of the used card brand on the generated radio map. In Section 4, the two testbeds presented used different APs and wireless NICs, and the results were consistent. This is because we do not assume a specific model for the signal strength, but rather we capture the behavior in the offline phase using the radio map. (2) The second and more challenging case is when a radio map built with one card is used for localization with another card. First, this is less severe than in the device-based case as the hardware involved in the device-free case is part of the system infrastructure and does not change with the person. If a hardware change occurs after the radio map has been constructed, then this problem can be addressed by some approaches that were discussed before in the context of the device-based localization [5].

7 Related Work

This section discusses relevant related work. We start by the device-based active localization systems followed by other device-free passive localization systems.

7.1 Device-based Active Localization

A number of systems has been introduced over the years to address the localization problem. These systems include the GPS system [3], ultrasonic-based systems [15],infrared-based systems [19], and RF-based systems [1]. All these systems share the requirement that the tracked entity needs to carry a device. In addition, many of these technologies require the device being tracked to actively participate in the localization process by running part of the localization algorithm. Moreover, some of these systems are limited in range due to the physical characteristics of the signal they use in localization.

Nuzzer allows entities tracking without them carrying any device nor participating actively in the localization process. In addition, *Nuzzer* works with the standard wireless data networks, and thus enhances the value of the data network. Since RF signals penetrate walls, *Nuzzer* does not require LOS and has good coverage range.

7.2 Device-free Passive Localization

A number of systems over the years have considered device-free passive localization, including radar based systems, and medical imaging based systems.

Ultrawideband (UWB) radar systems provide "Through-wall" detection and tracking. UWB radar systems can utilize impulse [22], frequency-modulated continuous-wave (FMCW) [18], stepped frequency [8], or noise [10] waveforms. These systems are very accurate, yet very complex. An alternate development is to use a Doppler radar with a two-element receiver array to provide less complexity [12]. This Doppler radar assumed that no two targets have the same Doppler return, which is not valid in case of human tracking since micro Doppler returns from the human arm and leg motions have a broad Doppler spread [4]. A four-element array radar can also be used [16]. This latter combines Doppler processing with software beamforming to resolve targets along both the Doppler and direction of arrival (DOA) space.

MIMO radar employs multiple transmit waveforms and has the ability to jointly process the echoes observed at multiple receive antennas (see [7] and references therein). Elements of the MIMO radar transmit independent waveforms resulting in an omnidirectional beampattern. It can also create diverse beampatterns by controlling correlations among transmitted waveforms. In MIMO, different waveforms are utilized and can be chosen to enhance performance in a number of ways.

In summary, radar-based systems are able to provide accurate location estimates. However, they require special hardware and their high complexity limits their applications.

	MIMO Radar-based Systems	**Radio Tomographic Imaging (RTI)**	***Nuzzer* System**
Measured Physical Quantity	Reflection and scattering	RSS attenuation	Changes in RSS
Range (based on frequency)	Short	Long	Long
Non-LOS localization	Yes	No	Yes
Number of deployed nodes (or devices)	Few	Many	Few
Complexity of single node (or device)	High	Low	Moderate
Number of streams	N/A (echo based)	Large (756)	Small (6)
Covering large areas	Limited by its short range (high frequency)	Limited by number of deployed nodes (LOS)	Yes
Accuracy	Very High	High	High
Accuracy degrades significantly with multipath	No	Yes	No
Handles multiple entities	Yes	Yes	Yes
Special hardware required	Yes	Yes	No
Substantial calibration efforts	No	No	Yes. Ongoing work
Licence-free frequency band	No	Yes	Yes

TABLE 3
Comparison of different RF-based passive localization systems

Another emerging technology is Radio Tomographic Imaging (RTI) [20]. It presents a linear model for using RSS measurements to obtain images of moving objects. The proposed system uses *hundreds* of raw data streams obtained from sensor nodes. The system measures the attenuation in the transmitted signal rather than scattering and reflection. Since this system is based on LOS, its accuracy degrades as multipath components increase. To overcome multipath, a higher density of nodes is used.

In [21], Wilson and Patwari presented a new method for imaging, localizing, and tracking motion behind walls. The method takes advantage of the motion-induced variance of RSS measurements made in a wireless peer-to-peer network. Using a multipath channel model, the authors show that the signal strength on a wireless link is largely dependent on the power contained in multipath components that travel through space containing moving objects. A Kalman filter is applied to recursively track the coordinates of a moving target. Experimental results for a 34-node through-wall imaging and tracking system over a 780 square feet area are presented.

The concept of *DfP* localization was first introduced in [27]. Experiments were set up in a highly *controlled* and small environment. In addition, the person was allowed to move in only one dimension. Results show that the system can track the intruder's position with more than 86% accuracy in this limited controlled environment. These results have established the proof of feasibility of the *DfP* concept. This has been further extended to a real environment, but still in a small scale, in [9].

The *Nuzzer* system has unique characteristics that differentiate it from the previous systems: It gives high accuracy for large-scale typical environments; it does not require any special hardware; it does not require LOS to operate; and it works with a low number of raw data streams. However, the current system has one main limitation: it needs substantial calibration efforts. This is being addressed in our ongoing work, as discussed in Section 6. Table 3 summarizes the differences between *Nuzzer* and recent *DfP* RF-based localization systems.

8 Conclusion

We presented the design, implementation, and evaluation of the *Nuzzer* device-free passive localization system. We evaluated the performance of the *Nuzzer* system both analytically and experimentally in two typical testbeds rich in multipath. Our results show that, for the first testbed, the *Nuzzer* system gives a median distance error of 1.82 meters, 3.7 times better than deterministic techniques and 7.7 times better than a random estimator. For the second testbed, the system gives a median distance error of 0.85m.

We also presented techniques based on the variance of the RSS to estimate the number of entities in the area of interest and localize them to coarse-grained zones. The techniques were evaluated in two different testbeds. For the first testbed, the proposed techniques can estimate the number of entities with 81% accuracy with the remaining 19% error always within a difference of one from the actual number of entities. Similarly, the system can identify the correct zone with 80% accuracy with the remaining error limited to adjacent zones. Similar results are obtained for the second testbed. We also showed how these techniques can enhance the scalability of the system significantly.

Currently, we are expanding the system in different directions including: automatic generation of the passive radio map, optimizing the APs and MPs positions, and analyzing the effect of dynamic changes in the environment and different hardware.

References

[1] P. Bahl and V. N. Padmanabhan, "RADAR: An In-Building RF-based User Location and Tracking System," in *IEEE Infocom 2000*, vol. 2, March 2000, pp. 775–784.

[2] P. Bahl, V. N. Padmanabhan, and A. Balachandran, "Enhancements to the RADAR user location and tracking system," Microsoft Research, Tech. Rep. MSR-TR-00-12, February 2000.

[3] P. Enge and P. Misra, "Special issue on GPS: The global positioning system," *Proceedings of the IEEE*, pp. 3–172, January 1999.

[4] J. L. Geisheimer, E. F. Greneker, and W. S. Marshall, "High-resolution doppler model of the human gait," *Proc. SPIERadar Sensor Technology and Data Visualization*, vol. Vol. 4744, pp. 8 –18, Jul. 2002.

[5] A. Haeberlen, E. Flannery, A. M. Ladd, A. Rudys, D. S. Wallach, and L. E. Kavraki, "Practical robust localization over large-scale 802.11 wireless networks." in *MOBICOM'04*, 2004, pp. 70–84.

[6] P. Hafezi, A. Nix, and M. Beach, "An experimental investigation of the impact of human shadowing on temporal variation of broadband indoor radio channel characteristics and system performance," in *Vehicular Technology Conference, 2000. IEEE VTS-Fall VTC 2000. 52nd*, vol. 1, Sep 2000, pp. 37–42.

[7] A. M. Haimovich, R. S. Blum, and L. J. Cimini, "Mimo radar with widely separated antennas," *IEEE Signal Processing Magazine*, pp. 116–129, January 2008.

[8] A. R. Hunt, "A wideband imaging radar for through-the-wall surveillance," *Proc. SPIESensors, and Command, Control, Communications, and Intelligence (C3I) Technologies*, vol. Vol. 5403, pp. 590 – 596, Sep. 2004.

[9] A. E. Kosba, A. Abdelkader, and M. Youssef, "Analysis of a device-free passive tracking system in typical wireless environments," in *the 3rd International Conference on New Technologies, Mobility and Security, NTMS 2009*, December 2009, pp. 1–5.

[10] C. P. Lai and R. M. Narayanan, "Through-wall imaging and characterization of human activity using ultrawideband (UWB) random noise radar," *Proc. SPIESensors and C3I Technologies for Homeland Security and Homeland Defense*, vol. Vol. 5778, pp. 186 – 195, May 2005.

[11] H. Lim, L. Kung, J. Hou, and H. Luo, "Zero-configuration, robust indoor localization: theory and experimentation," in *Proceedings of IEEE Infocom*, 2006, pp. 123–125.

[12] A. Lin and H. Ling, "Doppler and direction-of-arrival (DDOA) radar for multiple-mover sensing," *IEEE Trans. Aerosp. Electron. Syst.*, vol. Vol. 43, no. 4, pp. 1496 – 1509, Oct. 2007.

[13] R. J. Orr and G. D. Abowd, "The smart floor: A mechanism for natural user identification and tracking," in *Conference on Human Factors in Computing Systems (CHI 2000)*, The Hague, Netherlands, April 2000, pp. 1–6.

[14] J. D. Parsons, *The Mobile Radio Propagation Channel*. John Wiley and Sons Ltd, 2000.

[15] N. B. Priyantha, A. Chakraborty, and H. Balakrishnan, "The cricket location-support system," in *6th ACM MOBICOM*, Boston, MA, August 2000.

[16] S. S. Ram, Y. Li, A. Lin, and H. Ling, "Human tracking using doppler processing and spatial beamforming," *IEEE 2007 Radar Conference*, 2007.

[17] M. Seifeldin and M. Youssef, "Nuzzer: A large-scale device-free passive localization system for wireless environments," *arXiv:0908.0893v2, Arxiv.org*, August 2009.

[18] P. van Dorp and F. C. A. Groen, "Human walking estimation with radar," *Proc. Inst. Electr. Eng.Radar, Sonar Navig.*, vol. Vol. 150, no. 5, pp. 356 – 365, Oct. 2003.

[19] R. Want, A. Hopper, V. Falco, and J. Gibbons, "The active badge location system," *ACM Transactions on Information Systems*, vol. Vol. 10, no. 1, pp. 91–102, January 1992.

[20] J. Wilson and N. Patwari, "Radio tomographic imaging with wireless networks," *IEEE Trans. Mobile Computing*, 2009.

[21] ——, "Through-wall motion tracking using variance-based radio tomography networks," *Technical Report arXiv:0909.5417v2, arXiv.org*, Oct 2009.

[22] Y. Yang and A. E. Fathy, "See-through-wall imaging using ultra-wideband short-pulse radar system," *Proc. IEEE Antennas Propag. Soc. Int. Symp. Dig.*, vol. Vol. 3B, pp. 334–337, Jul. 2005.

[23] M. Youssef and A. Agrawala, "Small-scale compensation for WLAN location determination systems," in *IEEE WCNC 2003*, March 2003.

[24] ——, "The Horus WLAN Location Determination System," in *Third International Conference on Mobile Systems, Applications, and Services (MobiSys 2005)*, June 2005.

[25] ——, "The Horus location determination system," *ACM Wireless Networks (WINET) Journal*, 2007.

[26] M. Youssef, A. Agrawala, and A. U. Shankar, "WLAN location determination via clustering and probability distributions," in *IEEE PerCom 2003*, March 2003.

[27] M. Youssef, M. Mah, and A. Agrawala, "Challenges: device-free passive localization for wireless environments," in *MobiCom '07: Proceedings of the 13th annual ACM international conference on Mobile computing and networking*. New York, NY, USA: ACM, 2007, pp. 222–229.

[28] G. Zaharia, G. El Zein, and J. Citerne, "An experimental investigation of the influence of the moving people on the indoor radio propagation," in *Antennas and Propagation Society International Symposium, 1994. AP-S. Digest*, vol. 3, Jun 1994, pp. 1898–1901.

Moustafa Seifeldin received his M.Sc. in Communications and Wireless Technology from Nile University, Cairo, Egypt in 2010 and his B.Sc. in Electrical Engineering from Alexandria University, Alexandria, Egypt in 2008. He is currently working towards his Ph.D. in Electrical Engineering with the Wireless Networking and Communications Group (WNCG), the University of Texas at Austin, USA. His research interests include signal processing, wireless communications and cognitive radios.

Ahmed Saeed Ahmed Saeed is with the Egypt-Japan University of Science and Technology (E-JUST), Egypt. He received his B.Sc. in Computer and Systems Engineering from Alexandria University, Egypt in 2010. His research interests include networks scalability and utilization, wireless sensor networks and parallel computing. Saeed is a winner of the ACM SIGMobile 2009 undergraduate research competition.

Ahmed Kosba is with Alexandria University, Egypt. He received his B.Sc. in Computer and Systems Engineering from Alexandria University in 2009, and is currently preparing his M.Sc. in Computer Science in the same university. His research interests include location determination systems, pattern recognition and computer vision.

Amr El-Keyi was born in Alexandria, Egypt, in 1976. He received the B.Sc. (with highest honors) and M.Sc. degrees in Electrical Engineering from Alexandria University in 1999 and 2002, respectively, and the Ph.D. degree in 2006 in Electrical Engineering from McMaster University, Hamilton, ON, Canada. From November 2006 till April 2008, he was a postdoctoral research fellow with the Department of Electrical and Computer Engineering at McGill University. From May 2008 till February 2009, he was an Assistant Professor at Alexandria University where he participated in teaching several undergraduate courses. In April 2009, he joined Nile University as an Assistant Professor at the School of Communication and Information Technology. His research interests include statistical signal processing, array processing, cognitive radio, and cooperative relaying for wireless communication systems.

Moustafa Youssef is an Assistant Professor at Alexandria University and Egypt-Japan University of Science and Technology (E-JUST), Egypt. He received his Ph.D. degree in computer science from University of Maryland, USA in 2004 and a B.Sc. and M.Sc. in computer science from Alexandria University, Egypt in 1997 and 1999 respectively. His research interests include location determination technologies, pervasive computing, sensor networks, and network security. He has eight issued and pending patents. He is an area editor of the ACM MC2R and served on the organizing and technical committees of numerous conferences and published over 60 technical papers in refereed conferences and journals. Dr. Youssef is the recipient of the 2003 University of Maryland Invention of the Year award for his *Horus* location determination technology and the 2010 TWAS-AAS-Microsoft Award for Young Scientists, among others.